JOURNAL OF Applied Polymer SCIENCE

Biomimetic porous collagen/hydroxyapatite scaffold for bone tissue engineering

Li Chen,[1,2] Zhenxu Wu,[1,2] Yulai Zhou,[1] Linlong Li,[2,3] Yu Wang,[2,3] Zongliang Wang,[2,3] Yue Chen,[1] Peibiao Zhang[2,3]

[1]School of Pharmaceutical Sciences, Jilin University, Changchun 130021, People's Republic of China
[2]Key Laboratory of Polymer Ecomaterials, Changchun Institute of Applied Chemistry, Chinese Academy of Sciences, Changchun 130022, People's Republic of China
[3]University of Chinese Academy of Sciences, Beijing 100039, People's Republic of China
Correspondence to: Y. Chen (E-mail: cyue@jlu.edu.cn) or P. Zhang (E-mail: zhangpb@ciac.ac.cn)

ABSTRACT: Bone defect and osteochondral injury frequently occur due to diseases or traumatism and bring a crucial challenge in orthopedics. The hybrid scaffold has shown promise as a potential strategy for the treatment of such defects. In this study, a novel biomimetic porous collagen (Col)/hydroxyapatite (HA) scaffold was fabricated through assembling layers of Col containing gradual amount of HA under the assistance of "iterative layering" freeze-drying process. The scaffold presents a double gradient of highly interconnected porosity and HA content from top to bottom, mimicking the inherent physiological structure of bone. Owing to the biomimetic structure and component, significant increase of cell proliferation, alkaline phosphatase activity, and osteogenic differentiation *in vitro* was observed, illustrating potential application of the excellent Col/HA scaffold as a promising strategy for bone tissue engineering. © 2017 Wiley Periodicals, Inc. J. Appl. Polym. Sci. **2017**, *134*, 45271.

KEYWORDS: biomimetic; bone tissue engineering; collagen; composite scaffold; hydroxyapatite

Received 17 March 2017; accepted 30 April 2017
DOI: 10.1002/app.45271

INTRODUCTION

Bone defect is a common disease associated with functional disability that seriously affects the quality of life of patients, occurring frequently due to trauma, tumor, or other bone diseases.[1] Bone possesses particular ability of self-healing in some cases, while large bone defect probably do not heal spontaneously and surgical intervention is needed to prevent further degeneration.[2] The available bone substitutes used for clinical transplantation mainly include autologous bone, allograft bone, xenogenic bone, and synthetic materials like metals, ceramics, or polymers,[3] most of which have shown limited success and undesirable side effects in long-term repair.[4] In recent decades, the tissue engineering (TE) has emerged as a promising approach for orthopedic application with the advancement of nanotechnology and provides significant advantages compared with traditional clinical treatment methods.[4,5]

TE-based scaffolds have been proved to have great potential for regenerating a series of tissues and organs including bone, and could reduce the high failure rate of surgical reconstruction of large bone defect.[6,7] Natural materials, including collagen (Col),[8] fibrin,[9] hyaluronan,[10] alginate,[11] and agarose,[12] have been widely investigated for usage in bone tissue repair. Thereinto, the collagen offers particular advantages and has been incorporated with many other materials in order to improve their biological function. Besides, inorganic materials and synthetic polymers materials, such as hydroxyapatite (HA), poly(D,L-lactic acid-*co*-glycolic acid) (PLGA),[13] poly(L-lactic acid) (PLLA),[14] poly(propylene fumarate) (PPF),[15] poly(caprolactone) (PCL),[16,17] and a cyclic acetal hydrogel,[18] also have been widely used as bone-grafting materials.

The bone tissue of adult is composed of 2/3 of inorganic substance and 1/3 of organic component. And they mainly refer to the HA-like calcium salt composition and collagen.[19] HA [$(Ca_{10}(PO_4)_6(OH)_2$] has been widely used in bone TE because of its good biocompatibility, biodegradability, osteoconductivity, and non-toxicity.[20] Collagen is a primary component of extracellular matrix and provides an excellent basis for generating artificial substitutes for diseased or damaged bone tissues as it is readily available, nontoxic, and promotes the cellular process of proliferation, differentiation, adhesion, and migration.[21] Col/HA scaffold has become a hot spot of research in recent years because of its uniformity with bone tissue.[1,4,5,14,22] Al-Munajjed *et al.*[23] prepared biomimetic Col–HA scaffold using SBF immersion

J_ID: z8e Customer A_ID: APP45271 Cadmus Art: APP45271 Ed. Ref. No.: APP.20170454 Date: 20-May-17 Stage: Page: 2

technique and reviewed that this scaffold with improved mechanical properties and great biological performance can be used in bone TE properly. Rodrigues *et al.*[24] prepared Col–nanohydroxyapatite biocomposite scaffolds by cryogelation method and osteoblasts cells were able to attach and spread in all cryogels surfaces of scaffolds with higher cellular proliferation.

Structurally, the bone is composed of compact bone which is distributed on the surface with dense property and high pressure resistance, and spongy cancellous bone which is distributed within the bone woven by a large number of trabecula structure. The bone density should increase gradually from inside out. Levingstone *et al.*[5] developed a layered construct by the method enabling control over the properties of the construct. But this multi-layered scaffold did not fully achieved biomimetic function. We supposed that composite materials produced with collagen and HA by some technique should be an optimal choice for bone regeneration, mimicking the composition and structure of natural bone. Previously, our group investigated that highly interconnecting porous scaffold with a tunable pore structure could be fabricated by freeze-drying at different freezing temperature (4 °C, −20 °C, −80 °C, and −196 °C) and the average pore diameter varied from (167.2 ± 62.6) μm to (11.9 ± 4.2) μm.[25] So we got inspiration and applied the technique in the manufacture of scaffold. In this study, a biomimetic Col/HA composite scaffold with dual-gradient of HA content and pore size were fabricated through a simple "layer-by-layer" freeze-drying technique. The process involved repeated steps of layer addition followed by freeze-drying at different temperature levels (–20 °C, −80 °C, and −196 °C). The morphology and chemical properties of the composite scaffolds were characterized by environmental scanning electron microscopy (ESEM) and fourier transform infrared spectroscopy (FTIR). *In vitro* tests were performed using bone marrow mesenchymal stem cells (BMSCs) to determine biocompatibility of the scaffold, including cell attachment, proliferation, infiltration into the porous architecture, and distribution throughout the construct. Meanwhile, the effect of osteogenic differentiation of BMSCs was investigated through detection of alkaline phosphatase (ALP) activity and osteogenesis-related gene expression.

EXPERIMENTAL

Materials

Type I collagen was extracted from rat tail tendon using acid extraction method. HA was obtained from Nanjing Emperor Nano Material Co., Ltd (Nanjing, China). The reagents for cell experiments were purchased from Gibco (California, USA). Bovine serum albumin (BSA), 3-(4,5-dimethyl-2-thiazolyl)-2,5-diphenyl-2-*H*-tetrazolium bromide (MTT), and alizarin red-S (ARS) were obtained from Beijing Solar-bio Science & Technology Co., Ltd (Beijing, China). And *p*-nitrophenol phosphate substrate (pNPP) was purchased from Sigma–Aldrich (St. Louis, MO USA).

Collagen Purification

The use of rat-tail tendon for TE applications is well established in literature.[22] In this study, type I collagen was extracted from Sprague Dawley rat tail tendons in a manner similar to that described by Liu *et al.*[26] with modifications. Rat tail tendon was cut and suspended in 0.5 *M* acetic acid for 3 days at 4 °C. Then the insoluble residue was removed by centrifugation at 9000*g* for 60 min. The crude collagen was salted out from the supernatant by addition of 20% NaCl. The flocculent precipitate was collected by centrifugation at 9000*g*, for 60 min, then washed by 0.9% NaCl for three times to remove redundant NaCl. The precipitate was dissolved in 0.5 *M* acetic acid and dialysed in distilled water for 7 days at 4 °C. Finally, the purified collagen was obtained by lyophilization.

Scaffold Fabrication

The dual-gradient Col/HA scaffold was prepared with three different kinds of Col/HA suspensions. Briefly, rat tail tendon type I collagen was blended with 0.5 *M* acetic acid for 24 h under 4 °C environment using an overhead blender to a final collagen concentration of 1% (wt/vol).[27] The collagen solution was cross-linked using 0.05% glutaraldehyde at 4 °C for 3 h.[28] HA powder was suspended in distilled water and well distributed by ultrasonic treatment. The HA suspension was added into the cross-linked Col solution to obtain a final Col-HA ratio at 3:7 (wt/wt) and the mixture would be the lower layer suspension.[29] The intermediate layer and the upper layer suspension were composed by Col and HA with the final ratio of 5:5 (wt/wt) and 7:3 (wt/wt), respectively.[1]

Subsequently, the composite scaffold were fabricated through a simple "layer-by-layer" freeze-drying technique[5] involving repeated steps of layer addition followed by freeze-drying at different temperature levels. Briefly, the lower layer suspension was pipetted into a stainless-steel disc (internal diameter 20 mm) and subsequently placed into the −196 °C environment for 2 h. The frozen layer was taken out from the −196 °C environment for about 3 min before the intermediate layer suspension was pipetted under the lower layer and subsequently placed into the −80 °C environment for 2 h. The process described above was repeated for the two-layer scaffold prior to the addition of the upper layer suspension then the multi-layer scaffold was placed into the −20 °C environment for 2 h. Then it was freeze-dried at a final freezing temperature of −40 °C. Cubical scaffold samples were cut from the scaffold sheet for further experiments. In addition, the pure collagen scaffold was fabricated using the freeze-drying method as a control.

Scaffold Characterization

Microstructure of the scaffolds was examined by ESEM (Philips XL30 FEG). FTIR (Perkin Elmer, FTIR-2000) was used to determine the chemical structure of every layer of the scaffold and pure collagen scaffold.

Cell Culture and MTT Assay

In vitro analysis was carried out in order to assess scaffold biocompatibility, cellular attachment, and cell differentiation.[30] The scaffolds were cut into blocks with 20 mm in diameter and 6 mm in height. And then it was soaked in ethanol for 24 h and 0.1 *M* glycine solution for 1 h to eliminate glutaraldehyde and then washed by phosphate buffer saline (PBS) for three times. The scaffolds were sterilized by immersing in 75% ethanol for 2 h and washed by sterilized PBS for three times. Finally, the treated scaffolds were infiltrated in culture medium for 4 h before cell experiments.

ID: jwweb3b2server Time: 12:46 I Path: D:/Wiley/Support/XML_Signal_Tmp_AA/JW-APP#170431

J_ID: z8e Customer A_ID: APP45271 Cadmus Art: APP45271 Ed. Ref. No.: APP.20170454 Date: 20-May-17 Stage: Page: 3

Table I. Sequences of Primers for the qRT-PCR

Gene	Forward primer sequence (5′–3′)	Reverse primer sequence (5′–3′)
AGG	CAAGGACAAGGAGGTGGTG	GTAGTTGGGCAGCGAGAC
OPN	CGTGGATGATATTGATGAGGATG	TCGTCGGAGTGGTGAGAG
Col-I	CTCGCTCACCACCTTCTC	TAACCACTGCTCCACTCTG
Col-II	CTCAAGTCCCTCAACAACC	AG TAGTCACCGCTCTTCC
GAPDH	GATGGTGAAGGTCGGAGTG	TGTAGTGGAGGTCAATGAATGG

Two-week-old New Zealand white rabbits were used for BMSCs isolation and culture. BMSCs derived from bone marrow were cultured in basal medium, namely Dulbecco's modified Eagle's medium (DMEM) supplemented with 10% fetal bovine serum (FBS), 1% antibiotics, and incubated at 37 °C in a humidified 5% CO_2 atmosphere (standard condition). At almost 80% confluence, collected BMSCs(2×10^4) were seeded on each scaffold followed with addition of medium 4 h later and the cell-seeded scaffolds were incubated for 1, 3, and 7 days, respectively. The cell proliferation was detected by the standard MTT assay. Four hours before each culture interval, the culture medium was removed and the unattached cells were washed out with PBS solution for three times. About 100 μL of MTT (5 mg/mL in PBS) was added to each well, and the cells were incubated for an additional 4 h. Once completed, the medium was replaced by 800 μL of DMSO in each well to solubilize the converted dye. The solution (200 μL) in each well was mixed and transferred to a 96-well plate, and optical absorption was measured at 492 nm wavelength on a Full Wavelength MicroplateReader (Infinite M200, TECAN).

Cell Differentiation

ALP activity was detected to determine cell differentiation using *p*-nitrophenol phosphate substrate (pNPP) solution after cultured for 3, 7, and 10 days.[31] Briefly, the medium was removed carefully and cells were washed with PBS three times. The cells were lysed with Radio Immunoprecipitation Assay (RIPA) buffer, then frozen at −80 °C for 30 min.[32] Then pNPP solution was added and incubated in the dark at 37 °C for 30 min. The ALP activity was read on a Full Wavelength MicroplateReader (Infinite M200, TECAN) at 405 nm and the average optical density (OD) values were used to reflect the level of ALP activities correspondingly.

ARS staining was determined to detect the calcium deposition of BMSCs. After cultured for 21 days, the cell-seeded scaffolds were washed three times with PBS and fixed with 4% paraformaldehyde solution for 10 min. After washing three times with PBS, the cells were stained with ARS (50 m*M*) for 30 min at 37 °C.[33] Subsequently, the excess dye was washed off with distilled water, and all the scaffolds were photographed and examined. These scaffolds were immersed in 1 mL 10% hexadecylpyridinium chloride (CPC) at 37 °C for 1 h and calcium deposition activity was read on a Full Wavelength MicroplateReader (Infinite M200, TECAN) at 540 nm.[34]

Osteogenesis-Related Gene Expression

Cells were isolated from lower layer, intermediate layer, upper layer, the multi-layer scaffold, and pure collagen scaffold respectively, then total RNA was extracted from cells at 14 days. Phenol–chloroform extraction was performed using TRIzol reagent.[1] The levels of the mRNA for osteogenic specific genes, including Col-I, Col-II, aggrecan (AGG), and osteopontin (OPN), were assessed using real-time PCR.[35] The cDNA was synthesized using a PrimeScript™ RT reagent kit (Takara Bio, Japan) according to the manufacturer's instructions. All primer sequences were verified to be specific for target gene (Table I). T1
Quantification of osteogenic specific genes was tested using a Stratagene Mx3005p real-time PCR system with SYBR Green Mix Kit (TAKARA Biotechnology Co., Ltd.).[33] For quantitative real-time PCR, 10 μL of SYBR Premix Ex TaqTM, 6.8 μL of dH_2O, 0.4 μL of each forward and reverse primer, 0.4 μL of Rox, and 2.0 μL of cDNA template were used in a final reaction volume of 20 μL. The PCR amplification cycles included denaturation for 5 s at 95 °C, annealing, and extension for 34 s at 56 °C for 40 cycles. Data collection was enabled at 56 °C in each cycle. *Ct* (Threshold cycle) values were calculated using the Stratagene MxPro software v4.01 system. Each gene expression value was normalized to that of the housekeeping gene, glyceraldehyde-3-phosphate dehydrogenase(GAPDH). Results were reported as relative gene expression. All experiments were done in triplicate to obtain the average data.

Statistics Analysis

All data presented are expressed as the mean ± standard deviation. Statistical comparisons were carried out using analysis of variance (ANOVA) with the value of $P < 0.05$ being statistically significant ($^*P < 0.05$).

RESULTS AND DISCUSSION

The application of bone TE attracts more and more attention owing to the use of human stem cells and it would greatly improve the therapeutic strategies accordingly.[36] The TE scaffold could dispel the anxiety about autograft and allograft which are carrying problems of donor compatibility, supply limitation, pathogen transfer, and immune rejection.[37] We commonly think that an ideal scaffold should have an interconnecting porous structure with a diversity of end terminals (i.e., CH_3—, OH—), and biological properties such as biocompatible, non-immunogenicity, and biodegradability.[24] Collagen is a natural polymer extracted from various animals with poor mechanical property that limits its application enormously. HA is the most important and promising bioceramic material while HA only

ID: jwweb3b2server Time: 12:46 I Path: D:/Wiley/Support/XML_Signal_Tmp_AA/JW-APP#170431

J_ID: z8e Customer A_ID: APP45271 Cadmus Art: APP45271 Ed. Ref. No.: APP.20170454 Date: 20-May-17 Stage: Page: 4

COLOR ONLINE AND BW IN PRINT

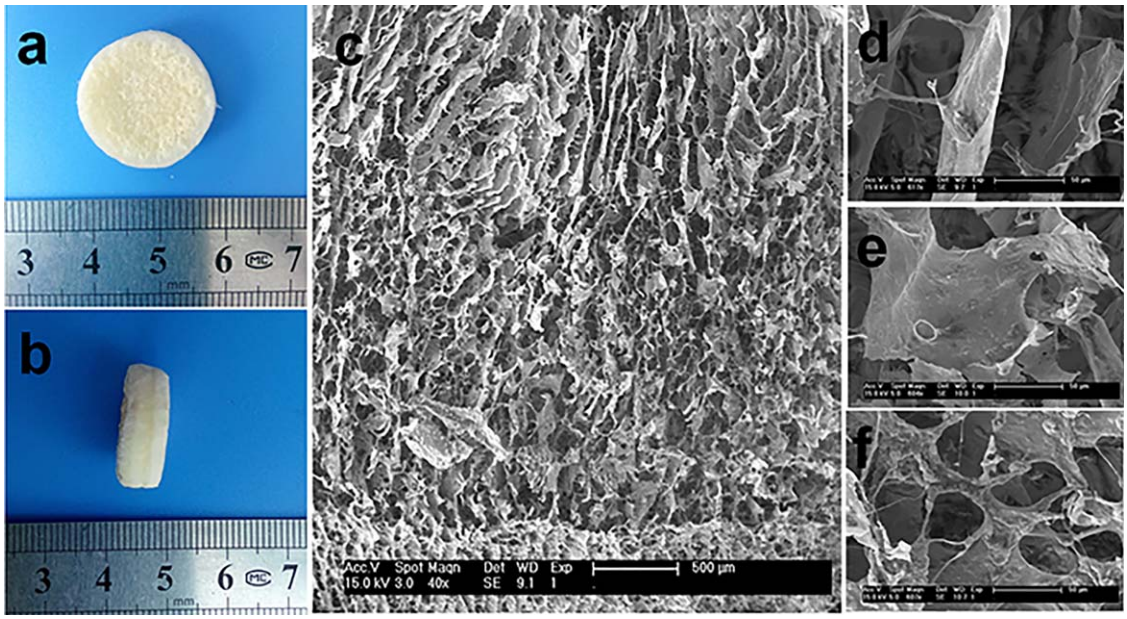

Figure 1. General appearance of the multi-layered Col-HA composite scaffold (a and b). ESEM micrographs of the multi-layered Col-HA composite scaffold (c, vertical section), the upper layer with the HA content of 30% (d), the intermediate layer with the HA content of 50% (e), and the lower layer with the HA content of 70% (f). [Color figure can be viewed at wileyonlinelibrary.com]

scaffold with high hardness and great brittleness couldn't form new bone in short-term. Our previous researches about HA confirmed that the HA is both biocompatible and osteoconductive.[30] The Col/HA composite materials, by mimicking the structure of natural bone, had become a focus of research in recent years. This composite materials exhibited superior mechanical properties, good biocompatibility, and osteoconductivity. And several studies showed that this composite could form calcification of bone matrix after mesenchymal stem cells inoculation.[2,22,37] The methods of preparation could be freeze-drying, mineralization method, SBF immersion technique, etc. The freeze-drying method is comparatively simple and practicable. Besides, previous studies in our laboratory showed that the average pore diameter of scaffolds created by lyophilization is changed at different freezing temperature.[25] So we prepared the Col/HA composite scaffold by "layer-by-layer" freeze-drying technique and got a dual-gradient biomimetic scaffold. The scaffold is an oblate cylinder, 20 mm in diameter, about 6 mm in high, and layers combined together closely with no gap between layers, as shown in Figure 1(a,b). F1

Morphology Analysis

The microstructure of the three-layer scaffold was demonstrated using ESEM analysis as shown in Figure 1. A high degree of pore interconnectivity throughout the construct was totally observed. The individual layers with respectively uniform porous structure were seamlessly integrated and the structural continuity at the interfaces was evident. This seamless integration of the scaffold layers is vital for promoting cell infiltration and regeneration of tissue in the different layers of the scaffold. The porous scaffold has bionic structure of bone with obviously different pore sizes and arrangement in each layer. The pore size was dependent on the freeze-drying parameters used in the fabrication process. To achieve a homogeneous pore structure, conduction of thermal energy between the material being freeze-dried and the freeze-dryer shelf is essential.[38] We prepared scaffold use the cylindrical stainless steel top-opening mold and freezing one layer followed by another layer covered. We observed that the hole array of upper and lower layer is more regular and orderly while the intermediate layer is messy and disorderly. Davidenko *et al.*[39] concluded that highly aligned matrices with axially directed pore architectures could be induced by single unidirectional temperature gradients. So we supposed that this microstructure maybe caused by the way of heat transfer. The freezing lower layer stunted energy transfer from the bottom side of stainless steel mold when the intermediate layer covered, disrupting the pore arrangement mode of intermediate layer. Image J software was used to measure the pore size of each layer and the average pore diameter of upper layer, intermediate layer, and lower layer are (132.36 ± 7.75) µm, (86.28 ± 7.96) µm, and (36.28 ± 5.72) µm, respectively. As expected, layered freezing enabled the control over pore size in each region of the construct so that the pore size gradually decreased and HA content gradually increased from top to bottom. Levingstone *et al.*[5] developed a multi-layer scaffold with seamlessly integrated layer structure. Progressively, our multi-layered scaffold with dual-gradient of HA content and pore size, by contrast, is more easily acquired by simple preparation method and more biomimetic with natural bone tissue. Besides, although the average pore size of lower layer is (36.28 ± 5.72) µm, this is enough for most cells such as osteoblasts and BMSCs to pass through pores, adhered the pore wall and proliferation.

FTIR Assessment

Infrared spectrum analysis of each layer of the scaffold is shown in Figure 2. The change of Col/HA composite was mainly in the range of 500–1800 cm^{-1}, while there was no significant F2

ID: jwweb3b2server Time: 12:46 I Path: D:/Wiley/Support/XML_Signal_Tmp_AA/JW-APP#170431

J_ID: z8e Customer A_ID: APP45271 Cadmus Art: APP45271 Ed. Ref. No.: APP.20170454 Date: 20-May-17 Stage: Page: 5

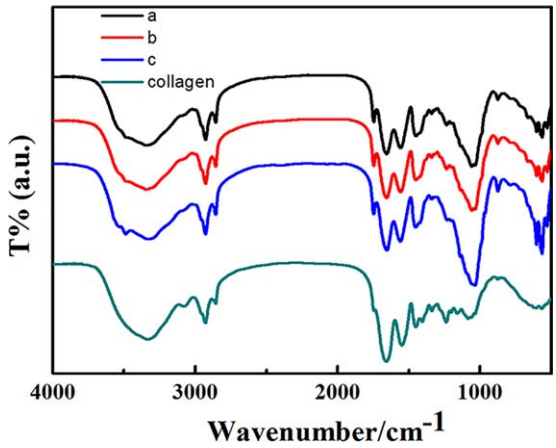

Figure 2. FTIR spectra of the upper layer composite (a), the intermediate layer composite (b), the lower layer composite (c), and the pure collagen scaffold. [Color figure can be viewed at wileyonlinelibrary.com]

change at 3300 cm^{-1} for the amino absorption peak (H—N stretching). Besides, stretching vibration for PO_4^{3-} group from HA was obtained at 1096 cm^{-1} for P—O stretch and at 573 cm^{-1} for P—O stretch coupled with P—O bend,[17] strong absorption peaks of PO_4^{3-} group can be seen at 1137, 900, and 566 cm^{-1}. According to the literature report, FTIR spectrum of collagen fibrils showed the typical amide bands such as N—H stretching at ~3305 cm^{-1} for the amide A, C—H stretching at ~3081 cm^{-1} for the amide B, C—O stretching at ~1635 cm^{-1} for the amide I, and N—H deformation at ~1545 cm^{-1} for the amide II,[20,40] stretching vibration for PO_4^{3-} group from HA was obtained at 1096 cm^{-1} for P—O stretch and at 573 cm^{-1} for P—O stretch coupled with P—O band.[17] The characteristic absorption band of collagen can be seen in every layer of Col/HA composites and stretching vibration for PO_4^{3-} group such as 560–570 cm^{-1} and 1000–1100 cm^{-1} for P—O bend also arisen. The variations of the FTIR spectra conformed that HA was successfully immobilized on the surface of collagen and there are no alterations in the collagen vibration mode after the HA was added.

Cell Proliferation

BMSCs were used to confirm the toxicity, biological activity, and differentiate property of the scaffold. MTT assay was carried out after culturing for 1, 3, and 7 days to investigate cell proliferation in scaffolds. As shown in Figure 3, the proliferation of BMSCs in collagen scaffold and Col/HA composite scaffold increased gradually with incubation time. The cell density in the Col/HA scaffold decreased a little at 3 days while there is a certain increase later and no significant difference was found between the two groups at 7 days post-seeding. The results indicated that the two scaffolds all have good biocompatibility, which can promote cell adhesion, growth, and proliferation. In addition, the cell density on the Col/HA scaffold was a little lower compared to the collagen scaffold at day 3 and day 7. Eosoly *et al.*[41] reported that composites with lower HA content showed the significantly higher cellular proliferation compared to that of higher HA content. Our result was similar to their reports that the collagen scaffold without HA showed a higher cellular proliferation. We suppose that the HA in the scaffold probably induced

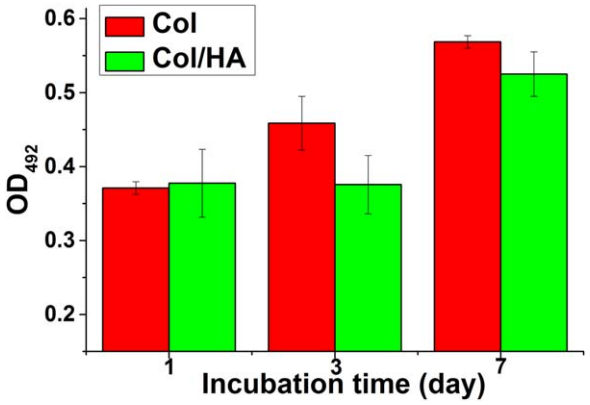

Figure 3. MTT test of BMSCs proliferation in the multi-layered Col/HA composite scaffold and the pure collagen (Col) scaffold for 1–7 days *in vitro*. [Color figure can be viewed at wileyonlinelibrary.com]

osteogenic differentiation of cells, therefore the cell proliferation has been depressed, and this hypothesis coincide with results of cell differentiation as aforementioned. It is reported that the addition of HA phase improve hydrophilicity of the scaffolds as well as change the surface roughness to make the scaffolds more bioactive and favorable for cell attachment.[42] Al-Munajjed *et al.*[23] developed a Col–HA scaffold using a SBF immersion technique and the scaffold with HA precipitation coated onto the collagen branch exhibit excellent biological performance. HA particulates on the collagen substrate could be observed in Figure 1(f) and this support cells adhesion and proliferation. No statistical difference in the cell proliferation could be seen after 7 days post-seeding between Col/HA scaffolds and pure collagen scaffolds, which suggests that the Col/HA scaffolds own excellent biological properties same as pure collagen scaffolds.

ALP Activity

ALP activity, which peaked during the pre-osteoblast stage of differentiation and is one phenotypic marker of osteoblasts,[33] was chosen to explore the osteoinductive activity of the Col/HA composites scaffold. Figure 4 shows the ALP activities of BMSCs in Col/HA scaffold and pure collagen scaffold at 3, 7, and 10 days. A great increase of ALP activity was found in the Col/HA

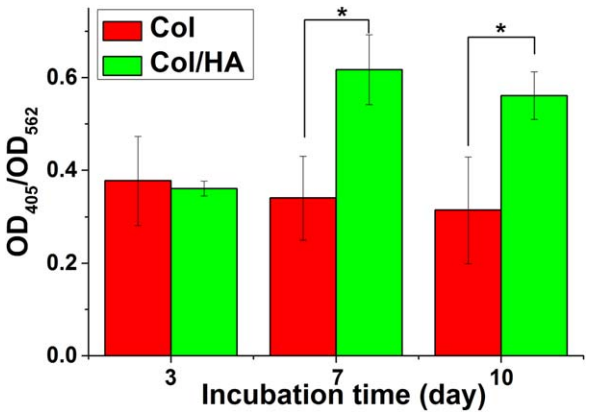

Figure 4. ALP activity of BMSCs in the different scaffolds for 3, 7, and 10 days analyzed with pNPP kit. $^*P < 0.05$, $n = 3$. [Color figure can be viewed at wileyonlinelibrary.com]

ID: jwweb3b2server Time: 12:46 I Path: D:/Wiley/Support/XML_Signal_Tmp_AA/JW-APP#170431

J_ID: z8e Customer A_ID: APP45271 Cadmus Art: APP45271 Ed. Ref. No.: APP.20170454 Date: 20-May-17 Stage: Page: 6

COLOR ONLINE AND BW IN PRINT

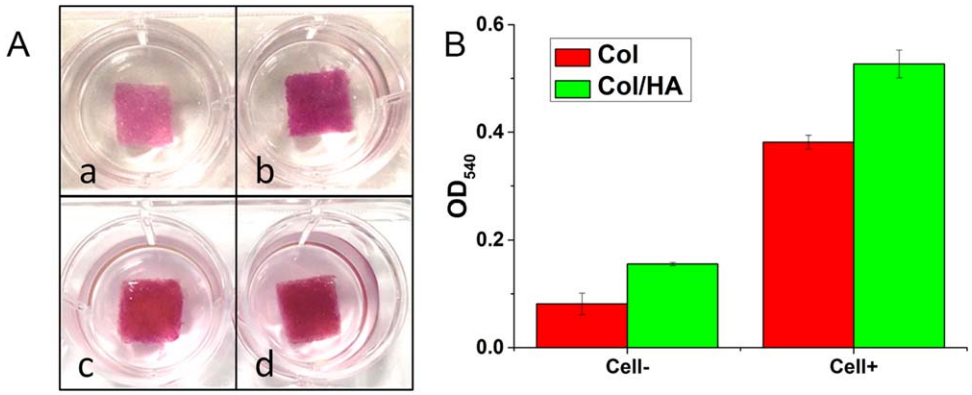

Figure 5. The results of Alizarin Red staining. ARS photographs of scaffolds (A). Collagen (Col) scaffold without BMSCs (a), Col/HA scaffold without BMSCs (b), collagen scaffold with BMSCs cultured for 21 days (c), Col/HA scaffold with BMSCs cultured for 21 days (d). Quantitative data of ARS (B). [Color figure can be viewed at wileyonlinelibrary.com]

scaffold, higher than those cells in collagen scaffold at 7 and 10 days. While the ALP activity of BMSCs in pure collagen scaffold decrease gradually with the time extended. The OD value of ALP activity in the Col/HAP scaffold was 84.2% and 78.8% higher than that in the pure collagen scaffold at 7 and 10 days, respectively, and statistical difference could be seen between the Col/HA scaffold and pure collagen scaffold. In our study, ALP activity had been normalized to the respective cell numbers and the results showed that although the starting number of cells present in the composite scaffold was far lesser than that in pure collagen scaffold, there was greater cellular activity of BMSCs in composite scaffold. The results of ALP activity in this two scaffolds showed that the composites scaffold exhibited stronger ability to promote BMSCs osteogenic differentiation than the pure collagen scaffold, owing to that HA could induce the osteogenic differentiation of BMSCs. It was reported that HA had positive influence on cellular behavior and mineralized scaffold induce greater cellular activity.[4] Meanwhile, it has been demonstrated that HA could induce the osteogenic differentiation of cells.[43] Akkouch *et al.*[42] reported that the type I collagen and HA were both found to enhance osteoblast differentiation and to accelerate osteogenesis. Our result confirmed this point that the Col/HA scaffold differentiate BMSCs and can promote bone formation to some extent.

ARS Staining

Sedimentary mineralization is the symbol of bone differentiation which indicated the bone cells are getting into the mineralization phase and mineralized extracellular matrix (ECM) was produced.[44] Osteogenic differentiation of BMSCs was induced in the composite scaffold. After 21 days of culture, the cells in both the pure collagen and composite scaffolds were treated by ARS which can bind to Ca^{2+} in mineralized ECM to examine calcium precipitation and mineralization. The scaffolds without cells seeding were also been treated as controls. Figure 5 was the optical images of ARS-stained scaffolds and significant difference was observed. The ARS staining was obviously visible in both pure collagen scaffold with cells and Col/HA scaffold with cells. While slight staining was found in pure collagen scaffold without cells and Col/HA scaffold without cells. Besides, the ARS staining of Col/HA scaffold with or without cells were both more significant than that in pure Col scaffold. Quantitative cell mineralization was performed by extracting ARS with 10% CPC to evaluate calcium-rich mineral deposits.[32] Normalized quantitative data with the scaffolds without cells, calcium quantification was recorded and the total calcium content in deposited minerals in Col/HA scaffold was about 24% higher than that in pure collagen scaffold. The transformation from BMSCs to osteoblasts is characterized by increased ALP activity and formation of calcified deposits. In our study, the total calcium content in deposited minerals in Col/HA scaffold was significantly higher than that in collagen scaffold. The same trend was observed in the quantitative cell mineralization with the ALP activity, it was further demonstrated that composite scaffold was capable of inducing cellular differentiation.[45]

Bone-Related Genes Expression

The relative gene expression of Col-I, OPN, AGG, and Col-II by BMSCs after 14 days of culture in the scaffolds was quantitatively analyzed using qRT-PCR and the results are shown in Figure 6. Collagen (mainly Col-I) is one of the main components of the natural bone ECM and the Col-I gene expression means that there was secretion of ECM by BMSCs. The result showed certain Col-I gene expression of BMSCs on each layer, multilayer composite scaffold and the pure collagen scaffold, illustrated that BMSCs were induced to produce extracellular matrix, thus promoting formation of bone tissue. OPN is an important tag for osteodifferentiation of BMSCs and the differentiation marker observed at the middle stage of differentiation along with the mineralization. Chen *et al.*[46] found that OPN plays a critical role in the lineage determination of MSCs and blockade of OPN function will suppress osteogenic differentiation while promoting robust adipogenic differentiation. A quantity of expression of OPN genes could be found in our results and this is just a more evidence for osteogenic differentiation. AGG and Col-II are important components of cartilage tissue secreted by cartilage cells. They are crucial markers for chondrogenic differentiation and their expression were important for endochondral ossification.[41,43–45] Our results showed that the composite scaffold and the pure collagen scaffold all have the potential for chondrogenesis of BMSCs but more data is needed to support this hypothesis. Interestingly, the results showed that

F5 F6

ID: jwweb3b2server Time: 12:46 I Path: D:/Wiley/Support/XML_Signal_Tmp_AA/JW-APP#170431

J_ID: z8e Customer A_ID: APP45271 Cadmus Art: APP45271 Ed. Ref. No.: APP.20170454 Date: 20-May-17 Stage: Page: 7

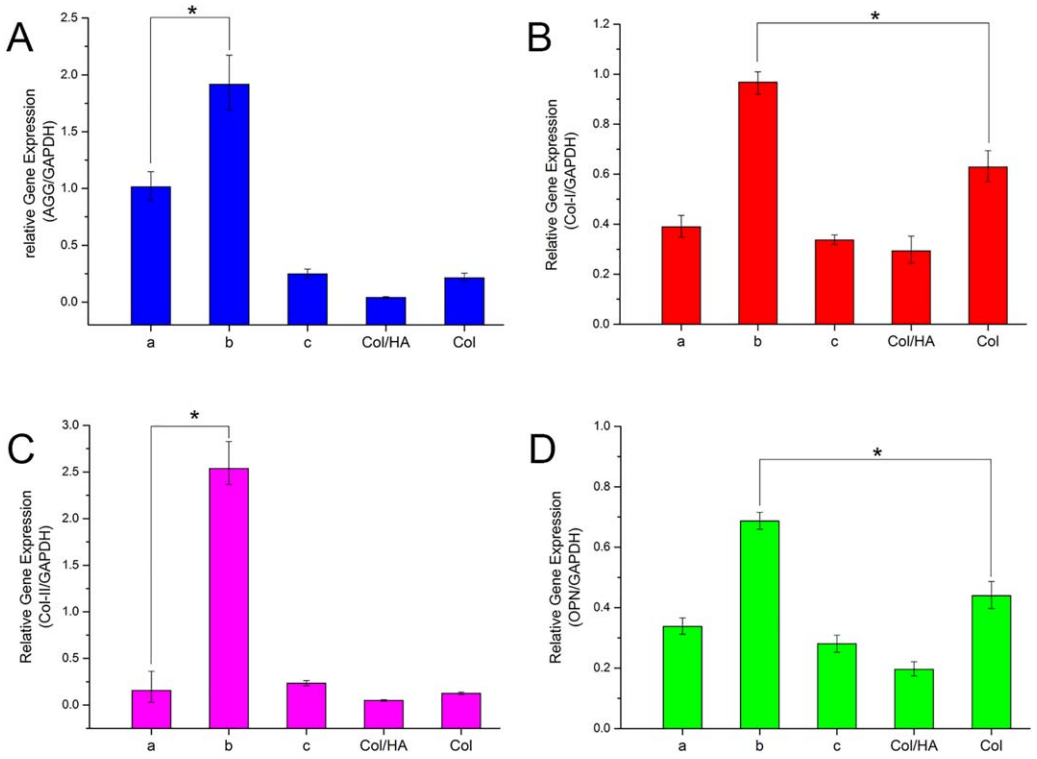

Figure 6. Quantitative real-time PCR analysis of osteogenesis-related gene expression of AGG (A), Col-I (B), Col-II (C), and OPN (D) after BMSCs cultured for 14 days. The expression level was normalized to that of the respective expression of GAPDH, which was used as a reference standard. The upper layer composite (a), the intermediate layer composite (b), the lower layer composite (c), $^*P < 0.05$, $n = 3$. [Color figure can be viewed at wileyonlinelibrary.com]

the gene expressions of BMSCs were highest when the cells were cultured in the intermediate layer scaffold (Col:HA = 5:5) compared to the cells in the upper layer (Col:HA = 7:3) and lower layer scaffold (Col:HA = 3:7). The multi-layered Col/HA scaffold did not show positive results. It indicated that HA could enhance the osteogenic differentiation of BMSCs and it is preferably in a suitable concentration.[43,45] In addition, current literature confirmed that addition of an intermediate level of HA can be beneficial,[41] while this will be determined in our future work.

CONCLUSIONS

In this study, a novel, seamlessly integrated Col/HA porous scaffold were developed by freeze-drying method and the resultant scaffold could mimic the inherent gradient structure of normal bone tissue with dual-gradient of HA content and pore size. This novel scaffold provided an optimized environment for cell attachment and proliferation due to a seamlessly integrated layer structure, high levels of porosity, a homogeneous pore structure, and a high degree of pore interconnectivity, all of which are essential in order to allow cellular infiltration, diffusion of nutrients, removal of waste, and to promote regeneration of seamless anatomical repair tissue. As a result, the proliferation of BMSCs in Col/HA composite scaffold was rapidly and ALP activities were higher compared to the pure collagen scaffold. Furthermore, the total calcium content in deposited minerals in Col/HA scaffold was significantly higher than that in collagen scaffold and relative genes expression of BMSCs is positive in Col/HA scaffolds. The result indicated that the composite scaffold had good biocompatibility and osteoconductivity that promote secretion of extracellular matrix and promoting formation of bone tissue. These results illustrated the potential of this double-gradient scaffold as an advanced strategy in bone TE.

ACKNOWLEDGMENTS

This research was financially supported by National Natural Science Foundation of China (Projects 51403197, 51473164, and 51273195), the Ministry of Science and Technology of China (International Cooperation and Communication Program 2014DFG52510), the joint funded program of Chinese Academy of Sciences and Japan Society for the Promotion of Science (GJHZ1519), and the Program of Scientific Development of Jilin Province (20170520121JH, 20130201005GX).

REFERENCES

1. Amadori, S.; Torricelli, P.; Panzavolta, S.; Parrilli, A.; Fini, M.; Bigi, A. *Macromol. Biosci.* **2015**, *15*, 1535.
2. Grassel, S.; Lorenz, J. *Curr. Rheumatol. Rep.* **2014**, *16*, 452.
3. Ma, B.; Xie, J. W.; Jiang, J.; Shuler, F. D.; Bartlett, D. E. *Nanomedicine (UK)* **2013**, *8*, 1459.
4. Ngiam, M.; Liao, S. S.; Patil, A. J.; Cheng, Z. Y.; Chan, C. K.; Ramakrishna, S. *Bone* **2009**, *45*, 4.

ID: jwweb3b2server Time: 12:46 I Path: D:/Wiley/Support/XML_Signal_Tmp_AA/JW-APP#170431

J_ID: z8e Customer A_ID: APP45271 Cadmus Art: APP45271 Ed. Ref. No.: APP.20170454 Date: 20-May-17 Stage: Page: 8

5. Levingstone, T. J.; Matsiko, A.; Dickson, G. R.; O'Brien, F. J.; Gleeson, J. P. *Acta Biomater.* **2014**, *10*, 1996.
6. Furth, M. E.; Atala, A.; Van Dyke, M. E. *Biomaterials* **2007**, *28*, 5068.
7. Uchida, N.; Sivaraman, S.; Amoroso, N. J.; Wagner, W. R.; Nishiguchi, A.; Matsusaki, M.; Akashi, M.; Nagatomi, J. *J. Biomed. Mater. Res. Part A* **2016**, *104*, 94.
8. Kane, R. J.; Roeder, R. K. *J. Mech. Behav. Biomed. Mater.* **2012**, *7*, 41.
9. Brittberg, M.; SjogrenJansson, E.; Lindahl, A.; Peterson, L. *Biomaterials* **1997**, *18*, 235.
10. Muzzarelli, R. A. A.; Greco, F.; Busilacchi, A.; Sollazzo, V.; Gigante, A. *Carbohydr. Polym.* **2012**, *89*, 723.
11. Igarashi, T.; Iwasaki, N.; Kasahara, Y.; Minami, A. *J. Biomed. Mater. Res. Part A* **2010**, *94*, 844.
12. Khanarian, N. T.; Haney, N. M.; Burga, R. A.; Lu, H. H. *Biomaterials* **2012**, *33*, 5247.
13. Sun, F.; Zhou, H.; Lee, J. *Acta Biomater.* **2011**, *7*, 3813.
14. Niu, X. F.; Feng, Q. L.; Wang, M. B.; Guo, X. D.; Zheng, Q. X. *J. Control. Release* **2009**, *134*, 111.
15. Lee, K. W.; Wang, S. F.; Yaszemski, M. J.; Lu, L. C. *Biomaterials* **2008**, *29*, 2839.
16. Heo, S. J.; Kim, S. E.; Wei, J.; Kim, D. H.; Hyun, Y. T.; Yun, H. S.; Kim, H. K.; Yoon, T. R.; Kim, S. H.; Park, S. A.; Shin, J. W.; Shin, J. W. *Tissue Eng. Part A* **2009**, *15*, 977.
17. Gupta, D.; Venugopal, J.; Mitra, S.; Giri Dev, V. R.; Ramakrishna, S. *Biomaterials* **2009**, *30*, 2085.
18. Patel, M.; Dunn, T. A.; Tostanoski, S.; Fisher, J. P. *J Tissue Eng. Regen. Med.* **2010**, *4*, 422.
19. Vallet-Regi, M. *J. Chem. Soc. Dalton* **2001**, 97.
20. Sionkowska, A.; Kozlowska, J. *Int. J. Biol. Macromol.* **2010**, *47*, 483.
21. Zhang, Y. F.; Cheng, X. R.; Wang, J. W.; Wang, Y. N.; Shi, B.; Huang, C.; Yang, X. C.; Liu, T. J. *Biochem. Biophys. Res. Commun.* **2006**, *344*, 362.
22. Panda, N. N.; Jonnalagadda, S.; Pramanik, K. *J. Biomater. Sci. Polym. Ed.* **2013**, *24*, 2031.
23. Al-Munajjed, A. A.; Plunkett, N. A.; Gleeson, J. P.; Weber, T.; Jungreuthmayer, C.; Levingstone, T.; Hammer, J.; O'Brien, F. J. *J. Biomed. Mater. Res. B* **2009**, *90*, 584.
24. Rodrigues, S. C.; Salgado, C. L.; Sahu, A.; Garcia, M. P.; Fernandes, M. H.; Monteiro, F. J. *J. Biomed. Mater. Res.. Part A* **2013**, *101*, 1080.
25. Xu, Y.; Zhang, D.; Wang, Z. L.; Gao, Z. T.; Zhang, P. B.; Chen, X. S. *Chin. J. Polym. Sci.* **2011**, *29*, 215.
26. Liu, X. D.; Skold, M.; Umino, T.; Zhu, Y. K.; Romberger, D. J.; Spurzem, J. R.; Rennard, S. I. *J. Lab. Clin. Med.* **2000**, *136*, 100.
27. Sionkowska, A.; Kozlowska, J. *Int. J. Biol. Macromol.* **2013**, *52*, 250.
28. Neethling, W. M.; Hodge, A. J.; Glancy, R. *J. Biomed. Mater. Res. Part B: Appl. Biomater.* **2003**, *66*, 356.
29. Flocea, P.; Popa, M.; Munteanu, F.; Verestiuc, L. *Rev. Med. Chir. Soc. Med. Nat. Iasi 113*, 286 **2009**.
30. Luo, B.; Choong, C. *J. Biomater. Appl.* **2015**, *29*, 903.
31. Shrivats, A. R.; Hsu, E.; Averick, S.; Klimak, M.; Watt, A. C.; DeMaio, M.; Matyjaszewski, K.; Hollinger, J. O. *Clin. Orthop. Relat. Res.* **2015**, *473*, 2139.
32. Gao, T. L.; Cui, W. W.; Wang, Z. L.; Wang, Y.; Liu, Y.; Malliappan, P. S.; Ito, Y.; Zhang, P. B. *RSC Adv.* **2016**, *6*, 20202.
33. Cui, H.; Wang, Y.; Cui, L.; Zhang, P.; Wang, X.; Wei, Y.; Chen, X. *Biomacromolecules* **2014**, *15*, 3146.
34. Lei, M.; Li, K.; Li, B.; Gao, L. N.; Chen, F. M.; Jin, Y. *Biomaterials* **2014**, *35*, 6332.
35. Cui, L. G.; Zhang, N.; Cui, W. W.; Zhang, P. B.; Chen, X. S. *J. Bionic Eng.* **2015**, *12*, 117.
36. Scaglione, M.; Fabbri, L.; Dell'Omo, D.; Gambini, F.; Guido, G. *Musculoskelet. Surg.* **2014**, *98*, 101.
37. Liu, X.; Ma, P. X. *Ann. Biomed. Eng.* **2004**, *32*, 477.
38. O'Brien, F. J.; Harley, B. A.; Yannas, I. V.; Gibson, L. *Biomaterials* **2004**, *25*, 1077.
39. Davidenko, N.; Gibb, T.; Schuster, C.; Best, S. M.; Campbell, J. J.; Watson, C. J.; Cameron, R. E. *Acta Biomater.* **2012**, *8*, 667.
40. Boskey, A.; Pleshko Camacho, N. *Biomaterials* **2007**, *28*, 2465.
41. Eosoly, S.; Vrana, N. E.; Lohfeld, S.; Hindie, M.; Looney, L. *Mater. Sci. Eng. C-Mater.* **2012**, *32*, 2250.
42. Akkouch, A.; Zhang, Z.; Rouabhia, M. *J. Biomed. Mater. Res. Part A.* **2011**, *96*, 693.
43. Gao, T. L.; Zhang, N.; Wang, Z. L.; Wang, Y.; Liu, Y.; Ito, Y.; Zhang, P. B. *Macromol. Biosci.* **2015**, *15*, 1070.
44. Xie, Q.; Wang, Z.; Zhou, H. F.; Yu, Z.; Huang, Y. Z.; Sun, H.; Bi, X. P.; Wang, Y. F.; Shi, W. D.; Gu, P.; Fan, X. Q. *Biomaterials* **2016**, *75*, 279.
45. Zhang, X. J.; Chang, W.; Lee, P.; Wang, Y. H.; Yang, M.; Li, J.; Kumbar, S. G.; Yu, X. J. *PLoS One* **2014**, *9*, e85871.
46. Chen, Q.; Shou, P. S.; Zhang, L. Y.; Xu, C. L.; Zheng, C. X.; Han, Y. Y.; Li, W. Z.; Huang, Y.; Zhang, X. R.; Shao, C. S.; Roberts, A. I.; Rabson, A. B.; Ren, G. W.; Zhang, Y. Y.; Wang, Y.; Denhardt, D. T.; Shi, Y. F. *Stem Cells* **2014**, *32*, 327.

ID: jwweb3b2server Time: 12:46 I Path: D:/Wiley/Support/XML_Signal_Tmp_AA/JW-APP#170431

SGML and CITI Use Only
DO NOT PRINT